



# Project 065(B) Fuel Testing Approaches for Rapid Jet Fuel Prescreening

## University of Illinois at Urbana–Champaign

### Project Lead Investigator

Tonghun Lee  
Professor of Mechanical Science & Engineering  
University of Illinois at Urbana–Champaign  
1206 W. Green St., Urbana, IL 61801  
517-290-8005  
[tonghun@illinois.edu](mailto:tonghun@illinois.edu)

### University Participants

#### University of Illinois at Urbana–Champaign (UIUC)

- P.I.: Professor Tonghun Lee
- FAA Award Number: 13-C-AJFE-UI-051
- Period of Performance: October 1, 2024, to September 30, 2025
- Tasks:
  1. Detailed Mixing and Chemistry Analysis for Lean Blowout (LBO) Evaluation
  2. Spray Characterization:
    - a. Analytical Model Techniques for Characterizing Combusting Sprays
    - b. Ignition Spray Measurements and Flame Propagation
    - c. Alternative Fuel Reduced Order Modeling (ROM) of Breakup Dynamics

### Project Funding Level

Federal Aviation Administration (FAA) funding level: \$150,000  
Cost Sharing: 100% matching funds provided by software license support from Converge, Inc.

### Investigation Team

Prof. Tonghun Lee, (P.I.), All Tasks  
Casey O'Brien, (graduate student), experimental efforts in characterizing the M1 combustor

### Project Overview

This study is aimed at introducing a new compact test rig (Army research combustor [ARC] M1), developed with original equipment manufacturer (OEM) support within the National Jet Fuel Combustion Program (NJFCP), that can screen fundamental combustor behavior with much lower fuel volumes (approximately gallons) before tier 3 and 4 tests in the ASTM D4054 (ASTM, 2024) evaluation. In the NJFCP, the referee rig at the Air Force Research Laboratory (AFRL) was used as a foundational test rig for this goal. The M1 may have the potential to perform screening tasks at reduced fuel volumes (approximately gallons rather than hundreds of gallons) in a simplified and open architecture that can be readily shared and operated at different locations at a fraction of the cost. Both the Army Research Laboratory (ARL) and Argonne National Laboratory (ANL) have been and will be partners in the effort to fully characterize the M1 facility. If successful, these efforts will allow fuel providers and OEMs to conduct basic combustor tests by using an identical testing architecture and identical test conditions at multiple test locations, in contrast to the referee rig, which is housed in a secure government facility (i.e., AFRL). Tests in smaller test rigs can provide a platform for individual suppliers or researchers to independently evaluate their new fuels and to make predictions without requiring the use of one single facility. Over time, as test data are accumulated, the potential for test rigs, such as the M1 to predict actual tier 3 and 4 performances will increase, potentially reducing the burden of relying on capital-intensive ASTM rig and engine tests.



### Background of the M1 Combustor

Under the FAA-funded NJFCP, the referee rig combustor at AFRL was used to determine the sensitivity of combustor performance parameters, such as LBO and ignition parameters, to the chemical composition of novel fuels. The results from this investigation were instrumental in establishing a relationship between fuel chemistry and its effects on combustor performance. Prof. Tonghun Lee's research group conducted a substantial portion of the laser and optical diagnostic work for the referee rig as part of the NJFCP, including quantitative-phase Doppler particle analysis, which provided key quantitative data for the simulation efforts.

Although the referee combustor used in the NJFCP program provides valuable information, a few key issues were identified. One issue is that the combustor requires hundreds of gallons of fuel to operate, which likely would not be available for many of the new sustainable aviation fuels (SAF) that would become available in the near future in the initial phase of production. The second issue is that the referee combustor lacks adequate optical access for diagnostics as a research combustor. Most significantly, it does not have windows on the top where laser beams can be inserted. Finally, the combustor itself is in a secure military facility (AFRL) and is not readily accessible to the general community. For these reasons, a smaller, compact, and less expensive option was needed; thus, the M1 combustor was developed with both the FAA and ARL (FAA NJFCP member). The M1 was designed as a joint effort between the University of Illinois and select OEMs who were involved with the referee combustor. The M1 combustor would run with moderately high-pressure air and would require a few gallons of fuel instead of hundreds of gallons. If this type of low-cost combustor can be well characterized, it can help prescreen SAFs as new fuels become available.

The dimensions and a magnified view of the M1 combustor are included in Figure 1. This combustor was built to be modular so that components can be easily switched out to suit the needs of different optical and laser diagnostics. The combustor includes four-sided optical access to allow for maximum flexibility in the diagnostics. The modular aspect was designed to allow us to transport the combustor easily to other locations for measurements, primarily because our team envisioned using x-ray imaging for fuel spray characterization at ANL as well as combustion characterization with velocity field and radical species measurements at UIUC. With this approach, the ASCENT Project 065(B) team can ensure that we are able to characterize the M1 combustor in an unprecedented way to enable wide adoption in the academic/industrial community as a test platform for new fuel blends. After this characterization is complete, the basic physics, dimensions, and operational envelope of the combustor will be openly shared with the academic and commercial sectors. This work is expected to provide a common platform not only for prescreening SAFs but also for performing other sustainability-related experiments involving novel fuels in a laboratory setting. It can also be noted that the combustor and surrounding hardware were designed specifically to be inexpensive (low flowrate requirements, lower pressure requirements, low fuel requirements on hardware) so that other labs could replicate this setup with reasonable resources.

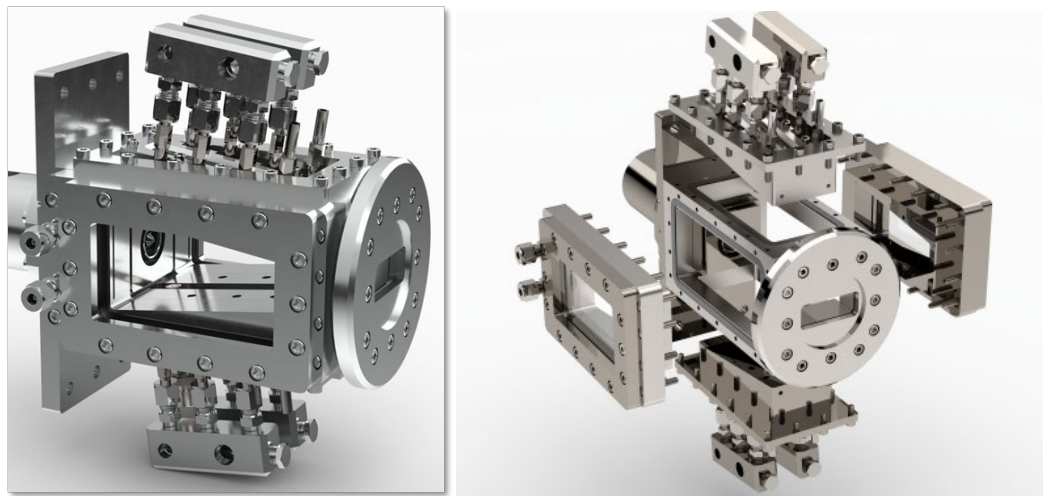


Figure 1. M1 combustor.



## Task 1 – Detailed Mixing and Chemistry Analysis for LBO Evaluation

University of Illinois at Urbana-Champaign

### Objectives

The main goal of this task is to find the direct causal link between fuel properties, in-flame fluid dynamics, and LBO performance. This work moves beyond simple correlation to determine why LBO behavior changes. A key objective is to determine if the flame structures, shear-layer instabilities, or heat release patterns are fundamentally different between the fuels, and if these differences can be used to predict LBO limits. To isolate these effects, LBO measurements are conducted on four fuels with wide-ranging properties at two combustor pressures. This pressure change is designed to force a transition from a physically dominated regime (where atomization and vaporization control LBO) to a chemically dominated one (where reaction kinetics are rate-limiting). By capturing this shift, it will be possible to pinpoint which specific fuel-driven dynamics are the limiting factors that control LBO under different conditions.

### Research Approach

Previous research, including large-scale tests within the NJFCP, successfully characterized LBO performance and established strong correlations between bulk fuel properties and LBO limits. However, these studies were largely focused on macroscopic behavior and often lacked the high-speed diagnostics required to understand the underlying mechanisms. Critically, they could not sufficiently resolve the transient flame-flow interactions, turbulent mixing, and flame dynamics that immediately precede a blowout event.

This research approach is designed to fill that specific knowledge gap. We are shifting the focus from if a fuel property affects LBO to how it does so at a fundamental, physical level. To achieve this, we are employing simultaneous 10 kHz OH-planar laser induced fluorescence (PLIF) and particle image velocimetry (PIV) imaging in the M1 combustor. This approach provides the high-fidelity, time-resolved data necessary to capture the detailed gas flow dynamics (i.e., PIV) and instantaneous heat release structures (OH-PLIF). This rich dataset is specifically intended for analysis with advanced ROM techniques. By applying methods like proper orthogonal decomposition (POD) and, in the future, dynamic mode decomposition (DMD), we can identify and quantify the dominant dynamic instabilities and coherent structures within the flame, allowing us to connect these specific physical phenomena directly to the LBO event. This allows us to move beyond simple correlation and build a model of the causal dynamic mechanisms that govern LBO for different fuels.

### Fuels for Lean Blowout Testing

In these experiments, four different fuels are tested in the M1 combustor to probe the effects of fuel properties on combustion behavior at these critical conditions. In addition to a reference fuel, the tested fuels consist of F-24 (comprising Jet A fuel and military-specific additives) and three fuels from the NJFCP with specific properties designed to probe the edges of the jet fuel operational envelope. Fuel C-1 has been developed with a low derived cetane number (DCN) and a relatively flat boiling curve. Fuel C-3 has been formulated to have a high viscosity, and fuel C-5 has been developed with an extremely flat boiling curve with respect to those of other fuels. Table 1 shows selected important parameters of each fuel for comparison, demonstrating some of the key features of the fuels chosen for testing.

Table 1. Comparison of key properties of the four tested fuels.

Fuel	Key features	Derived cetane number	Heat of combustion (MJ/kg)	H/C ratio	Stoichiometric air/fuel ratio	Kinematic viscosity at 40°C (cSt)	Surface tension (dynes/cm)
F-24	Jet A with additives	48.6	43.2	1.94	14.70	1.36	23.6
C-1	Low cetane	17.1	43.8	2.18	15.03	1.53	21.0
C-3	High viscosity	47.0	43.3	1.97	14.65	1.78	24.2
C-5	Flat boiling	39.6	43.0	1.94	14.68	0.83	22.2

### Previous Lean Blowout Results

A principal component analysis (PCA) was used to overcome multicollinearity in fuel properties, reducing them to three key components: physical dependence (PD), chemical dependence (CD), and droplet dependence (DD). These components were correlated with LBO data at two pressures, revealing a clear regime transition shown in Table 2 and Figure 2. At 2 atm, LBO



is physically dominated, with the LBO equivalence ratio ( $\phi_{LBO}$ ) correlating strongly with properties governing atomization and vaporization, specifically the 20% distillation temperature ( $T_{20}$ ) and kinematic viscosity ( $\nu$ ). This was confirmed as the best-performing fuel, C-5, had low viscosity, while the worst-performing, C-3, had high viscosity. Increasing the pressure to 3 atm causes a distinct shift to a chemically dominated regime. At this pressure, the influence of physical properties diminishes, and the DCN becomes the most influential parameter. This transition occurs because the enhanced mixing and faster reaction kinetics at higher pressure mean that chemical reactivity (i.e., ignition delay), not atomization, becomes the rate-limiting step.

**Table 2.** Lean blowout (LBO) equivalence ratio ( $\phi_{LBO}$ ) correlation analysis with fuel properties for two pressures.

Noz	P (kPa)	TAFR (g/s)	$\phi_{LBO}$ (F-24)	$\phi_{LBO}$ (C-1)	$\phi_{LBO}$ (C-3)	$\phi_{LBO}$ (C-5)
A	203	65.07	0.173	0.167	0.188	0.147
B	203	65.07	0.104	0.104	0.106	0.097
C	203	65.07	0.149	0.133	0.157	0.125
B	304	92.18	0.066	0.084	0.065	0.064



**Figure 2.** Lean blowout (LBO) equivalence ratio correlation analysis with fuel properties for two pressures.

### Detailed Flame Mixing Characteristics

Detailed flame mixing characteristics for the four tested fuels were investigated using simultaneous 10 kHz OH-PLIF and PIV imaging. This approach allowed for the analysis of gas flow dynamics (PIV) alongside instantaneous heat release (OH-PLIF), a key indicator of combustion intensity. As shown in the average OH PLIF images (Figure 3), a clear differentiation in the flame structure and peak heat release location was observed among the fuels, despite similar average velocity fields across all four. Specifically, Fuel C-3, with its high viscosity, exhibited its peak heat release furthest downstream, followed sequentially by C-1, F-24, and C-5. This downstream shift of the flame front is almost directly correlated with the increasing kinematic viscosity of the fuels, confirming that physical properties significantly influence flame stabilization at these conditions.

Further insights into the dynamic behavior were gained by applying POD to both the PIV and PLIF fields. This method identifies the most energetic spatial structures (modes) within the data. By projecting the time-series onto these modes,



their temporal coefficients are extracted, allowing the energy contained within each dynamic mode to be quantified. This analysis revealed significant differences in the transient flow structures among the fuels. Notably, in some of the lower-energy POD modes (e.g., mode 3 for PIV and mode 4 for PLIF), the high-viscosity fuel C-3 displayed much more pronounced instabilities within the upper outer shear layer, an instability that was considerably weaker in the other fuels. Figure 4 visually highlights this localized, energetic instability in the C-3 fuel. While POD effectively identified these key spatial structures and provided a crucial link between fuel viscosity and flame dynamics, its energy-based nature is less suited for defining the complete time-evolving system. Therefore, future work will leverage advanced ROM techniques, such as DMD, to more fully characterize these complex, time-dependent dynamics.

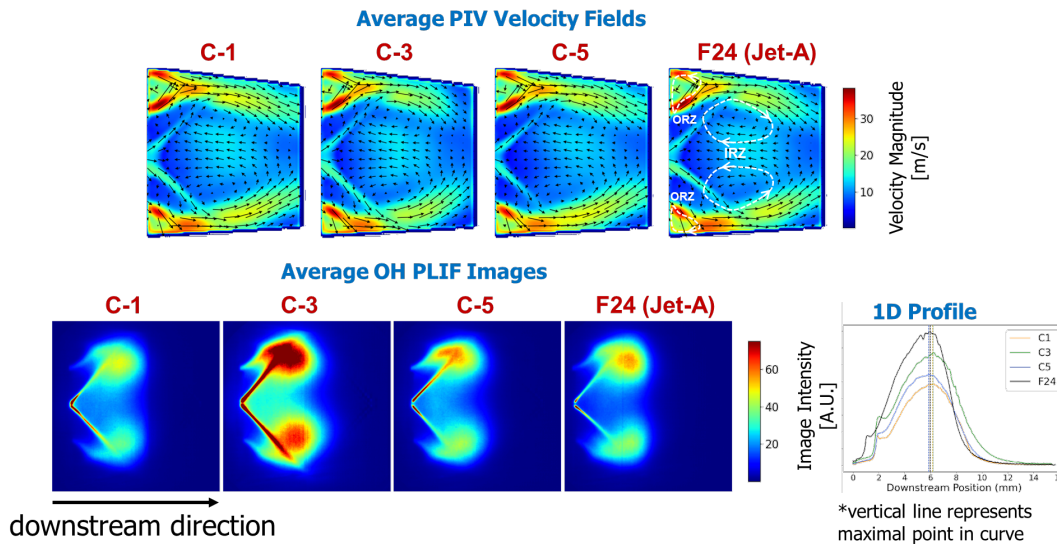


Figure 3. Average planar laser induced fluorescence (PLIF) particle image velocimetry (PIV) fields for four fuels.

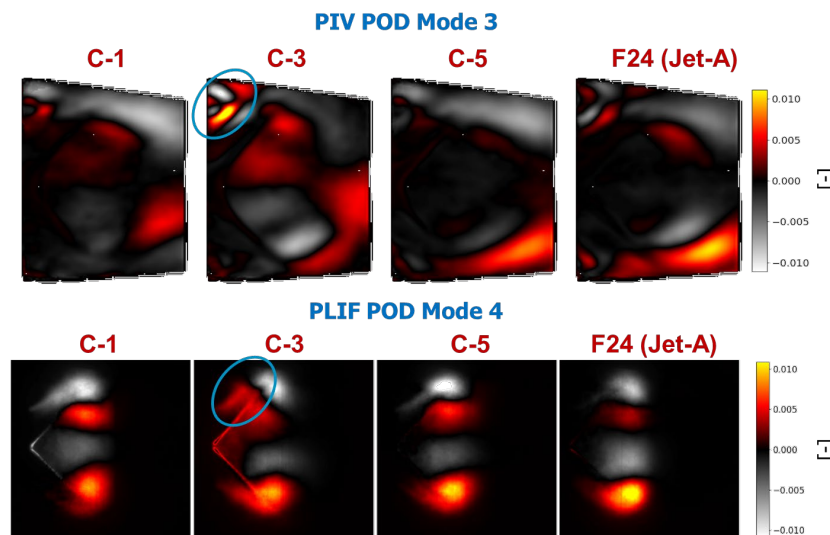


Figure 4. Lower energy modes identifying instabilities of planar laser induced fluorescence (PLIF) particle image velocimetry (PIV) through proper orthogonal decomposition (POD).



## **Milestones**

- Processed the high-speed diagnostic data to identify the dominant spatial modes and dynamic structures (6 months).
- Established the direct link between the diagnostic findings and the performance data. This involved correlating the ROM-identified dynamic features (e.g., shear layer instability strength) and mean-flow structures (e.g., flame standoff distance) with the LBO limits (12 months).

## **Major Accomplishments**

The major accomplishment of this investigation is the identification of the key causal mechanism linking fuel physical properties to LBO performance. This work has successfully moved beyond the correlations of previous studies by providing direct diagnostic evidence of how fuel properties fundamentally alter flame dynamics. The high-speed analysis revealed critical findings: average OH-PLIF fields show that high-viscosity fuels (e.g., fuel C-3) produce a longer flame standoff distance, pushing the primary heat release zone further downstream. The POD analysis then confirmed that this downstream flame position drives a pronounced hydrodynamic instability in the outer shear layer (Figure 4), a dynamic feature that was weak or absent in the other fuels. This instability is identified as the direct physical mechanism responsible for the degraded LBO performance of high-viscosity fuels.

## **Publications**

### **Published Conference Proceedings**

Dasgupta, D., & Som, S. (2024). Fuel property impact on lean blow out for sustainable aviation fuels in gas turbine combustors. *Proceedings of the ASME Turbo Expo 2024: Turbomachinery Technical Conference and Exposition. Volume 3A: Combustion, Fuels, and Emissions*, V03AT04A073, London, United Kingdom. <https://doi.org/10.1115/GT2024-126789>

Wood, E. J., Mayhew, E., Motily, A., Temme, J., Kweon, C. B., & Lee, T. (2021). Lean blowout dependence on fuel properties and combustion conditions in the ARC-M1 single-cup swirl combustor. AIAA 2021-0652. *AIAA Scitech 2021 Forum*. 0652. <https://doi.org/10.2514/6.2021-0652>

## **Outreach Efforts**

All test data will be made accessible through <https://altjetfuels.illinois.edu/>.

## **Awards**

None.

## **Student Involvement**

Task 1 was primarily conducted by Casey O'Brien (PhD student).

## **Plans for Next Period**

The primary focus for the next period will be to advance the ROM of the flame dynamics, moving beyond the spatial structure identification of POD. The high-speed OH-PLIF and PIV datasets will be analyzed using DMD. This analysis is central to extract the key spatiotemporal modes, their frequencies, and their growth/decay rates. The objective is to build a quantitative, dynamics-based model that directly links the amplitude and persistence of specific instabilities, such as the observed shear layer mode, to LBO performance.

This validated modeling framework will then be applied to an expanded set of alternative fuels. New tests will incorporate a wider range of fuel types, including hydroprocessed esters and fatty acids (HEFA), synthetic paraffinic kerosene (SPK), and alcohol-to-jet (ATJ) blends. This effort is not simply to expand the LBO database, but to test the generality of the identified mechanisms. This will provide a systematic framework to determine if the same controlling dynamics govern LBO for these new fuels or if their unique properties introduce different physical or chemical pathways to blowout.



## Task 2 – Spray Characterization

### Task 2a – Analytical Model Techniques for Characterizing Combusting Sprays

University of Illinois at Urbana–Champaign

#### Objectives

In this task, a novel, high-fidelity analytical framework is developed and validated to quantitatively characterize the primary breakup and spray dynamics in a combustor environment. This framework is necessary because traditional or single-point diagnostics are insufficient to resolve the complex, transient, and multi-scale physics of atomization, which is a rate-limiting step for fuel-air mixing. This work will combine high-speed X-ray phase contrast imaging (PCI) with a newly developed machine learning optical flow model, PC-Flow, to extract time-resolved velocity fields. The primary objectives are to (1) validate PC-Flow's performance and quantify its predictive uncertainty and (2) deploy this validated tool to establish new, physically-based metrics for spray characterization, including breakup time and sphericity evolution. By establishing this quantitative methodology, we provide the toolset required to isolate the physical properties (viscosity, surface tension, and volatility) of fuel variability on spray formation, which is essential for the subsequent ignition and fuel-comparison studies in Tasks 2b and 2c.

#### Research Approach

High-speed X-ray PCI was performed on the operating ARC-M1 combustor at stable combustor with a specific focus on the fuel spray immediately after exiting the nozzle. The experiments were performed using the X-ray white beam at ANL's Advanced Photon Source using beamline 7-BM. The ARC-M1 combustor was fitted with thin X-ray transparent Kapton windows to enable the beam to pass through the combustor. The technique allowed visualization of only the liquid fuel droplets in the combustor, enabled through a combination of X-ray absorption by the fuel and additional diffractions at the boundaries due to the density difference between the fuel and surrounding air. Figure 5 shows an image of important features of the ARC-M1 combustor as well as the imaging regions measured experimentally. The combustor conditions for the spray measurements were maintained at an inlet air temperature of 323 K and a combustor operating pressure of 1 atm. Two pressure drops across the combustor were tested. For the 26, 30, 35 g/min fuel flow rates, a 1.75% pressure drop was set, which resulted in 16.1 g/s main and 4.0 g/s dilution air flow rates. For the 37, 40, 45 g/min flow rates, a 3% pressure drop was set, resulting in 21.3 g/s main and 5.4 g/s dilution air flow rates. These specific pressure drops were selected to emulate the operating conditions of the referee rig, ensuring direct comparability between the two setups. Furthermore, relatively ambient conditions were utilized to establish a baseline dataset where the effects of pressure and inlet air temperature on droplet distribution are minimized.

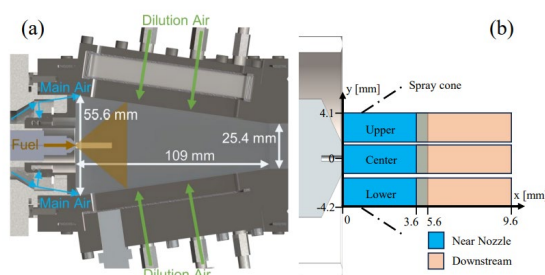


**Figure 5.** Schematics of (a) ARC-M1 combustor geometry and (b) imaging region.

We developed PC-Flow, an unsupervised machine learning optical flow model, to extract high-fidelity velocity fields from high-speed spray imaging. It builds on the UPFlow (state-of-the-art) architecture but integrates key modifications, including a new correlation volume, concatenated features to model flow dependencies, and an integrated attention mechanism. The UPFlow model performed best on publicly available synthetic datasets (KITTI 2012 & 2015) and consequently was chosen as baseline. The new design proved highly effective, demonstrating a 29.9% reduction in mean absolute error (MAE) compared to the original UPFlow baseline. Qualitatively, PC-Flow also produces less noisy velocity predictions that are well-localized to the liquid fuel structures shown in Figure 6. To ensure its suitability as an analytical instrument, we performed

a Lucas-Kanade-based uncertainty quantification (UQ). This validation confirmed that PC-Flow achieves sub-pixel average uncertainty for its velocity predictions shown in Figure 7, verifying its reliability for extracting quantitative physical data.

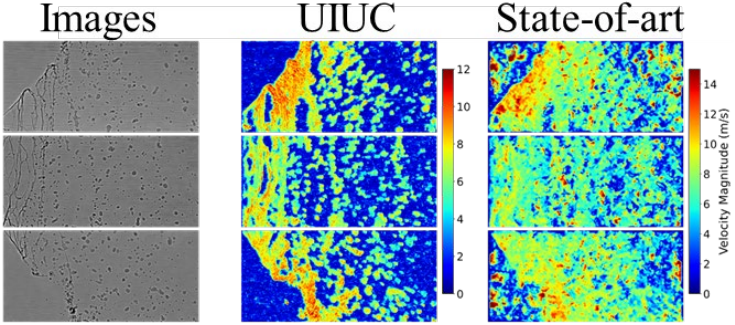


Figure 6. An example comparison of flow predictions: (a) raw images, (b) PC-Flow, and (c) UPFlow.

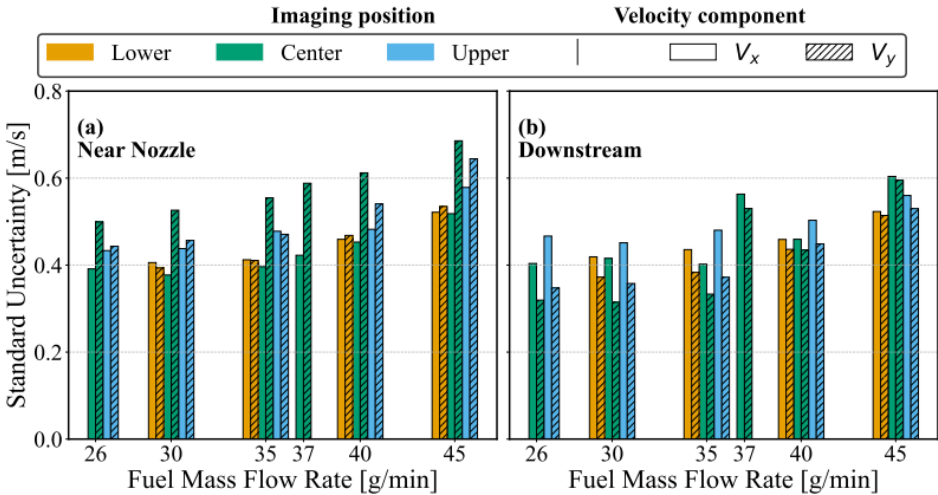
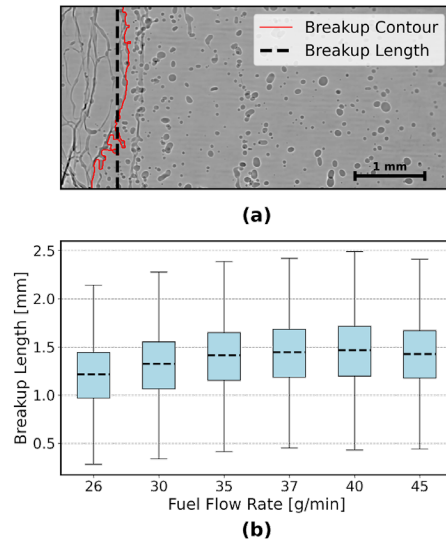


Figure 7. Average uncertainty estimation for multiple fuel flow rates and imaging positions: (a) near nozzle and (b) downstream.

Using this validated PC-Flow tool in conjunction with image binarization, we characterized the spray's primary breakup dynamics. A key parameter in any spray model is the primary breakup length ( $l_b$ ), as this location (visualized in Figure 8[a]) defines the critical transition from a continuous liquid sheet to discrete droplets. This, in turn, sets the initial conditions for all downstream processes, including vaporization, fuel-air mixing, and subsequent combustion. We tracked the leading edge of the liquid sheet (Figure 8[b]) and found that  $l_b$  increases near linearly with the fuel flow rate. However, the velocity data from PC-Flow provided a much deeper insight: by calculating the characteristic breakup time ( $\tau_b = l_b/V_x$ ), we found this value remained nearly constant. This strongly suggests that the leading edge breakup is governed by a fixed instability-driven rate, and the observed increase in length is primarily a transport-driven phenomenon where the faster-moving sheet simply travels further before it has time to disintegrate.



**Figure 8.** Breakup length estimation: (a) identification of the breakup point and (b) box plot of breakup length dispersion (dashed line indicates arithmetic mean, blue box indicates the interquartile range (Q1 to Q3), and vertical whiskers indicate the minimum and maximum values).

To understand the output of this breakup process, we analyzed the probability density functions (PDF) of velocity and droplet size, sampled at the breakup location (shown in Figure 9). This statistical approach is crucial because it moves beyond simple averages to capture the full operational range, which is essential for understanding spray consistency and the stochastic nature of ignition and other combustor tests. The velocity PDFs (Figure 9[a], Figure 9[b]) quantify the axial and transverse momentum being imparted to the new droplets, which governs their downstream penetration and mixing with the surrounding air. The droplet diameter PDF (Figure 9[c]) is a direct input for any vaporization or combustion model, as it defines the initial surface area available for heat and mass transfer.

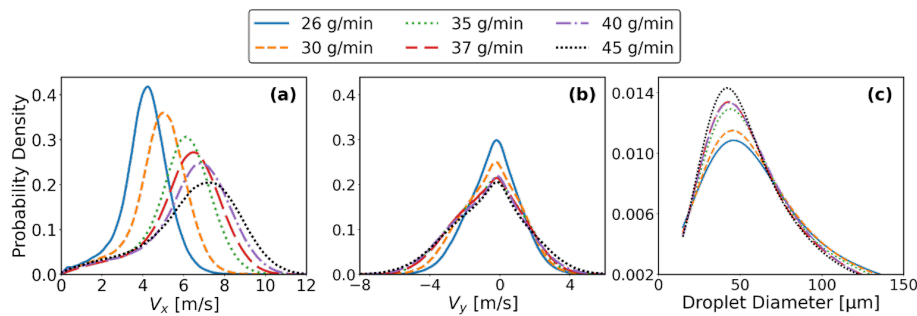


**Figure 9.** Probability density function at the breakup location of different fueling rates for (a)  $V_x$ , (b)  $V_y$ , and (c) droplet diameter.

Finally, we analyzed droplet sphericity as a function of downstream distance shown in Figure 10. This metric is critical for two primary reasons. First, many standard spray diagnostic techniques, such as phase doppler particle anemometry (PDPA), rely on the assumption of spherical droplets; our analysis directly quantifies where in the spray this assumption becomes valid (i.e., where sphericity approaches 1). This is vital for validating data used in certification. Second, the evolution of sphericity physically represents the spray's relaxation from chaotic, non-spherical liquid fragments into stable droplets, a process governed by the competition between aerodynamic shear (deforming the droplets) and surface tension (restoring them to spheres). We identified the inflection point of the sphericity curve as a new, physically meaningful metric that tracks the sheet's internal instability timescale (e.g., disintegration via perforation). This offers a powerful,



complementary perspective to the convective timescale captured by leading-edge tracking. Coupling this morphological data with PC-Flow's velocity data, we also discovered a slightly trimodal transverse velocity ( $V_x$ ) distribution near the chaotic breakup region. This is a direct signature of the highly fluctuating motion inherent to atomization, which transitions to a more developed, smoother flow as the droplets stabilize downstream.

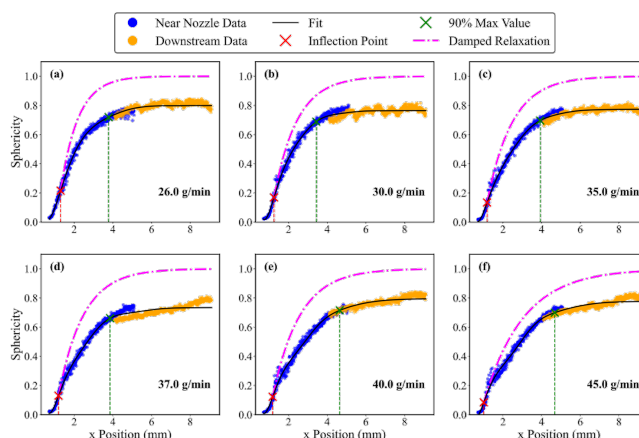


**Figure 10.** Sphericity curve along the streamwise direction: (a) 26 g/min, (b) 30 g/min, (c) 35 g/min, (d) 37 g/min, (e) 40 g/min, and (f) 45 g/min.

## Task 2b – Ignition Spray Measurements and Flame Propagation

University of Illinois at Urbana–Champaign

### Objectives

In this task, the transient spray dynamics governing gas turbine ignition and relight are investigated. This is a critical safety metric, as ignition is a stochastic process highly dependent on the local fuel droplet distribution at the spark kernel, particularly under low-load conditions. A knowledge gap persists in an in-situ quantification of the spray's response to the spark and subsequent flame. This study will use simultaneous high-speed X-ray PCI and broadband visible imaging to capture spark-droplet interactions and flame kernel propagation at relevant ignition conditions. The primary objective is to test the hypothesis that combustion itself alters the spray, by segregating and comparing spray statistics (e.g., D10 and D32) from pre-ignition (non-combusting) and post-ignition (combusting) sequences. We will determine whether preferential vaporization ( $D^2$  law) is the dominant mechanism downstream and whether thermal feedback from the flame front alters primary atomization near the nozzle. Understanding this quantitative link between spray properties and ignition success is essential for evaluating the relight performance of future SAFs, which may possess different vaporization characteristics than conventional jet fuel.

### Research Approach

Gas turbine ignition performance is a critical safety metric, particularly the ability to relight after a flame blowout, which can occur during low-load conditions like descent. Ignition is a stochastic process where a spark kernel's heat release must overcome local heat losses, a balance governed by the local droplet distribution and fuel-air mixture. Foundational research identified the quantity of fuel vapor from the spark as the critical factor. However, a knowledge gap persists regarding the transient dynamics of spark kernel interactions with liquid fuel droplets, particularly their vaporization. Resolving this interaction is crucial for low-temperature conditions where liquid-phase behavior dominates. This study investigates these transient phenomena in the ARC-M1 combustor at relevant low-load ignition conditions (25°C inlet air, atmospheric pressure). To capture the critical spark-droplet interactions, simultaneous broadband and high-speed X-ray PCI images are acquired. Both imaging systems are synchronized with a 4 Hz aviation spark igniter, with data acquisition commencing approximately 5.5 ms before each spark. This method yielded 750 broadband and 3,000 X-ray PCI images per sequence, enabling analysis of transient vaporization and kernel development. For statistical analysis, three pre-ignition and four spark sequences starting from ignition are consolidated, as depicted in Figure 11.

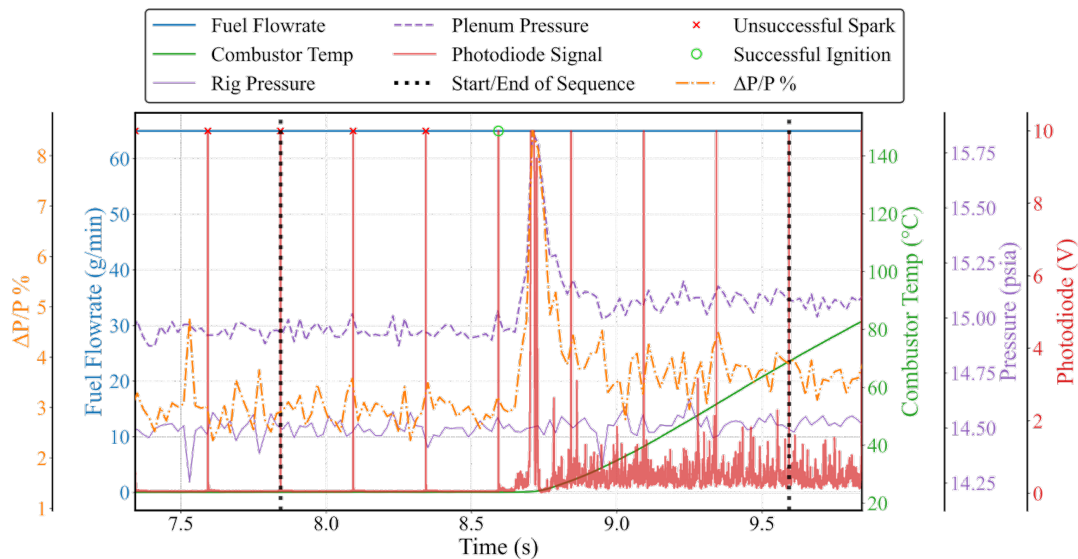


**Figure 11.** Temporal evolution of key metrics during sample ignition test at a fuel flowrate of 65 g/min. Recording sequence is highlighted with three sparks before ignition and four sparks starting from ignition.

### Combusting vs Non-Combusting Statistical Comparison

Droplet size distributions significantly impact gas turbine engine performance. Different statistical moments of the distribution are required to fully characterize spray behavior. The general form for a droplet size diameter based on statistical moments is:

$$D_{xy} = \left[ \frac{\sum n_i d_i^x}{\sum n_i d_i^y} \right]^{1/(x-y)}$$

where  $x$  and  $y$  define the moments and  $n_i$  is the number of particles with diameter  $d_i$ . The arithmetic mean,  $D_{10}$ , is the statistical mean of the number-weighted distribution. It represents the simple average diameter based on droplet count. Yet, the Sauter mean diameter  $D_{32}$ , which represents the diameter of a droplet with the same volume-to-surface-area ratio as the entire spray, is a standard metric used for correlating heat and mass transfer phenomena because these processes are highly dependent on total surface area.

To quantify discrete particle sizes, droplets were identified and extracted from each frame and then segregated into pre-combusting and post-combusting sequences. The raw histogram data were fitted to a truncated log-normal distribution, which provides a non-biased fit by accounting for droplets below the 10.8  $\mu\text{m}$  X-ray detection limit. A log-normal distribution is physically appropriate, as droplet breakup is a multiplicative cascade process that trends toward this distribution via the central limit theorem. Figure 12 shows an example fit for both non-combusting and combusting sequences.

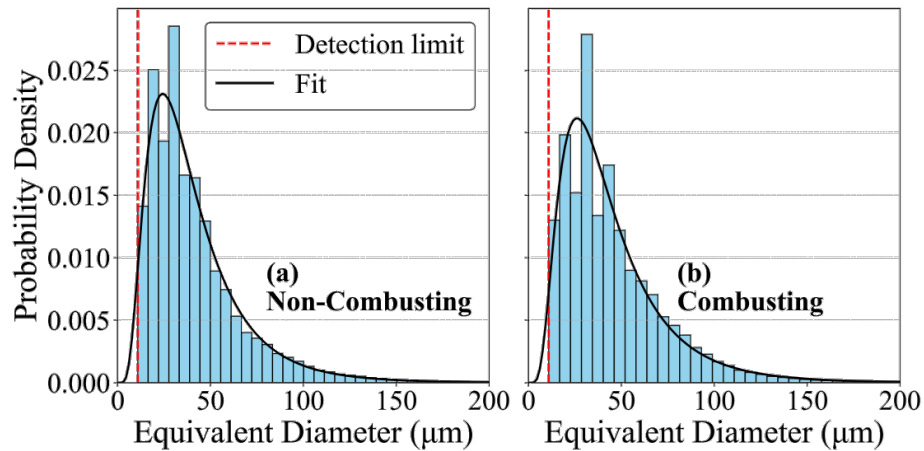


**Figure 12.** Histogram of measured droplet equivalent diameters with log-normal fitting: (a) non-combusting and (b) combusting.

To compare general trends, Figure 13 plots  $D_{10}$  and  $D_{32}$  for combusting and non-combusting cases. The data cover two configurations, near-nozzle ( $x=0$  mm) and downstream ( $x=12$  mm), and two different pressure-swirl nozzles (Nozzle A and Nozzle B). Nozzle A is the same as that used in Section 2a. At the downstream position ( $x=12$  mm), the  $D_{32}$  is noticeably larger in the combusting case, while the  $D_{10}$  is simultaneously smaller. This combined trend is a strong indicator of preferential vaporization, consistent with the  $D^2$  evaporation law. The smallest droplets, which have the highest surface-area-to-volume ratio, evaporate fastest. The decrease in  $D_{10}$  indicates that the increased vaporization is reducing the overall population, lowering the simple average diameter of all droplets. However,  $D_{32}$  becomes larger because it is now biased toward the remaining, larger droplets that dominate the spray's total surface area.

The near-nozzle position ( $x=0$  mm) shows a more complex phenomenon, where both  $D_{10}$  and  $D_{32}$  are larger for the combusting case. At this position, there has been insufficient time for droplet evaporation to be the primary cause of this size increase. This implies that the combustion process itself is altering the primary atomization dynamics. Thermal feedback from the flame front to the liquid sheet, or modified aerodynamics from gas expansion, likely changes the liquid's breakup characteristics.

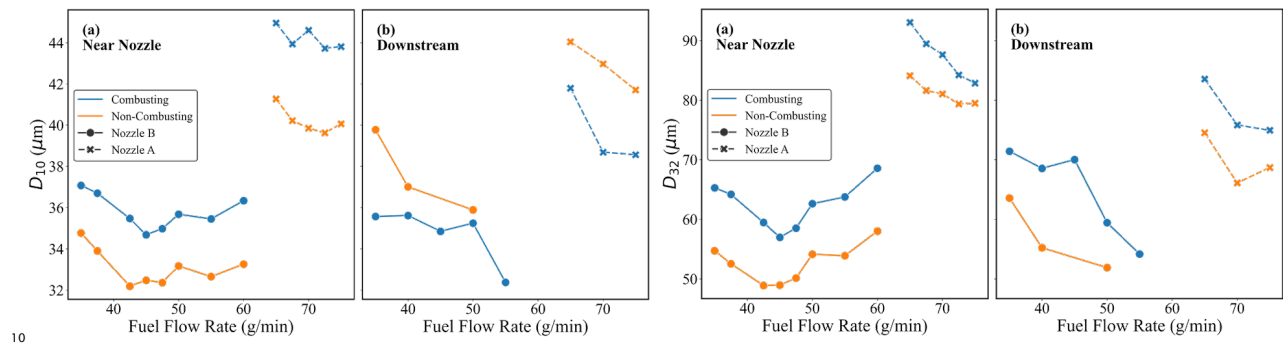


**Figure 13.** Mean diameter of fitted droplet distributions for non-combusting and combusting cases: (a) near nozzle and (b) downstream.

In addition to droplet distributions, the integrated behavior of flame propagation is analyzed. Flame propagation is captured via high-speed broadband visible imaging, and the flame extent is determined using a binarization scheme. Figure 14 summarizes the intensity-weighted centroid movement over time for unsuccessful (non-combusting) and successful (combusting) ignition events. For this analysis, time is normalized so that ignition occurs at  $t=0$  seconds. In



unsuccessful cases, the centroid positions are scattered. In successful cases, this behavior transitions, with the centroid swirling and then attracting to a central region. Future analysis will focus on correlating the flame extent and propagation dynamics with local droplet properties.

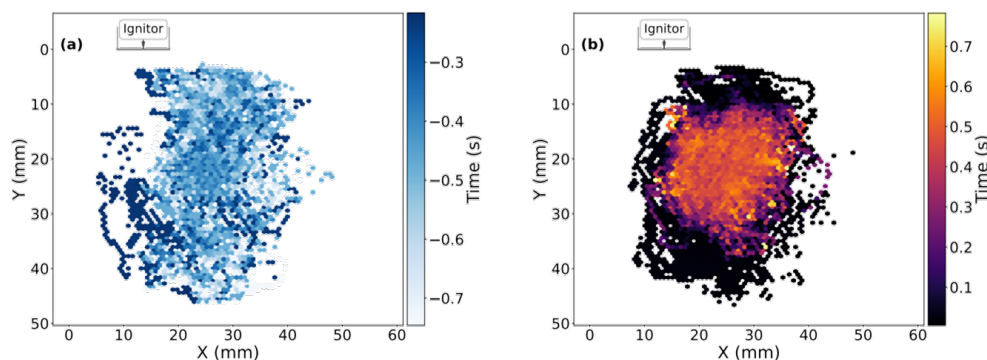


Figure 14. Flame kernel weighted centroid propagation: (a) non-combusting and (b) combusting.

## Task 2c – Alternative Fuel Reduced Order Modeling of Breakup Dynamics

### University of Illinois at Urbana-Champaign

#### Objectives

In this task, the impact of fuel property variability on primary atomization is directly investigated to accelerate the adoption of alternative fuels. The current ASTM D4054 certification process is a major bottleneck; developing "prescreening" tools that link fuel properties to spray performance is essential. This work will apply the validated analytical framework from Task 2a to a matrix of four fuels (F-24, C-1, C-3, C-5) selected for their wide-ranging physical properties (e.g., viscosity, distillation curve). We hypothesize that these properties create unique, quantifiable signatures in the spray's spatiotemporal velocity field. The primary objective is to use ROM, specifically DMD, to extract the dominant, low-dimensional physics from this high-dimensional data. This will provide a physically interpretable model that links specific fuel properties (like viscosity) to dominant breakup instabilities (e.g., spatial growth rates of DMD modes). This work represents a critical step toward creating a model-based prescreening methodology, reducing the reliance on large-scale, expensive testing for SAF certification.

#### Research Approach

ROM is an essential tool for quantifying dominant, translatable physics. Even in highly turbulent environments, ROMs can extract low-dimensional dynamics from seemingly random processes. This capability is critical for accelerating the adoption of alternative aviation fuels, which are necessary for sustainability and multi-fuel capability. Prescreening fuels by modeling their spray dynamics is therefore essential to reduce this cost and timeline. In smaller combustors, the time and length scales for atomization, vaporization, fuel-air mixing, and chemical reaction are shortened. Atomization and vaporization, in particular, become rate-limiting steps under unfavorable conditions, making spray behavior a key area of study.

Understanding the variance in spray dynamics across different fuels is therefore paramount. Classically, liquid sheet breakup is described via dispersion relations, where breakup is governed by the growth rate of the most unstable infinitesimal disturbance. However, this theory is difficult to validate experimentally, as it requires high-resolution spatiotemporal data. While some efforts have applied modal analysis to raw spray images of the liquid sheet (Leask et al., 2021; Jia et al., 2023; Kang et al., 2018; Kasmaiee et al., 2024), pixel intensity variance is not directly interpretable and does not necessarily correlate to physical motion or true variance. Therefore, it is more physically meaningful to pose the modal analysis in terms of the extracted velocity fields. Additionally, limited experimental work has investigated the effect of varying fuel properties on instability growth on the liquid sheet and breakup.



This analysis was accomplished using the optical flow model developed in Task 2a. Four different fuels with widely varying properties, shown in Table 1, are experimentally investigated: a baseline fuels F-24, C-1 (low cetane number), C-3 (high viscosity), and C-5 (low viscosity, flat boiling curve). Preliminary analysis on identical conditions to (Task 2a), but extended to these four fuels, indicates significant deviations in primary breakup length as identified by leading-edge contour tracking (Figure 15). Viscosity, a damping factor for deformation, appears to have a significant impact on breakup characteristics. Future work will involve using ROM to describe the breakup process. DMD is a promising methodology to coherently represent spatiotemporal information. This eigen decomposition technique has been applied to simulation data of spray breakup. Previous work suggests that temporal growth is not significantly meaningful in a pseudo-steady-state system. However, the spatial growth rates of individual modes may be a better indicator of instability. Preliminary dynamic mode decomposition of the four fuels shown in Figure 16 indicates spatial coherence in the axial direction indicating instabilities. Future work will investigate the DMD modeling technique for spray breakup prediction using this four-fuel dataset.

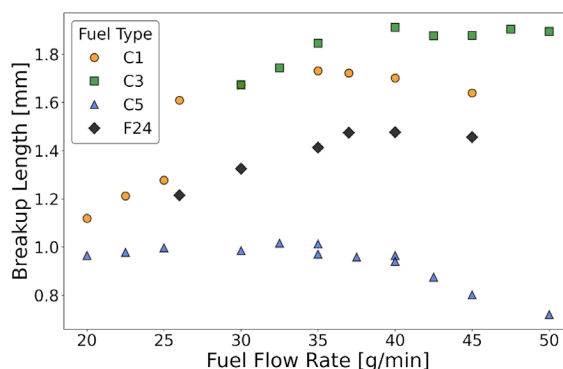


Figure 15. Primary breakup length of four fuels.

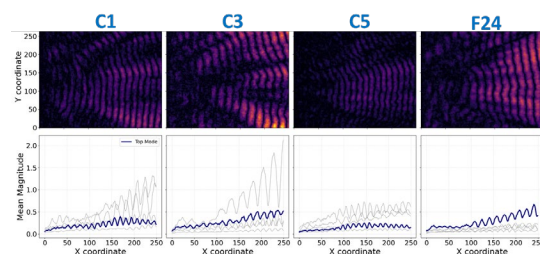


Figure 16. Dynamic mode decomposition spatial growth for four fuels.

### Milestones

- Developed optical flow PC-Flow model with uncertainty quantification for spray velocimetry (3 months).
- Characterization of field parameters for primary and secondary atomization (breakup length, sphericity, size, and velocity distributions) (6 months).
- Analysis of ignition spray measurements (9 months).
- Application of DMD to extract spatiotemporal instabilities for four fuels (12 months).

### Major Accomplishments

This research establishes a quantitative, mechanism-based framework for prescreening SAFs, addressing a key bottleneck in their certification. This is accomplished by moving beyond simple correlations to link fuel properties directly to in-situ spray dynamics under reacting conditions. First, a novel analytical tool, PC-Flow, was developed and validated to extract time-resolved velocity fields from combusting X-ray spray data, providing the necessary quantitative metrics (Task 2a). This framework was then applied to ignition, providing direct evidence that the combustion process itself actively alters



atomization and drives preferential vaporization, demonstrating that non-reacting spray data are insufficient for predicting performance (Task 2b). Finally, this validated methodology is now being applied to a matrix of fuels with diverse properties. By coupling these high-fidelity velocity fields with ROM (i.e., DMD), this work will produce a physically-interpretable, low-dimensional model that links specific fuel properties (e.g., viscosity) to quantifiable breakup instabilities (e.g., DMD spatial growth rates), forming the basis of a predictive prescreening tool for new SAFs (Task 2c).

## **Publications**

### **Peer-Review Journal Articles**

O'Brien, C. J., Kang, K., Wood, E. J., Yoon, J., Mayhew, E. K., Kastengren, A., Kweon, C. M., & Lee, T. (2026). Time-resolved spray characterization via unified optical flow and binarization technique. *Fuel*, 407(C), doi: 137433.

<https://doi.org/10.1016/j.fuel.2025.137433>

Oh, J. H., Wood, E., Mayhew, E., Kastengren, A., & Lee, T. (2023). Sequence2Self: Self-supervised image sequence denoising of pixel-level spray breakup morphology. *Engineering Applications of Artificial Intelligence*, 126(B), doi: 106957.

<https://doi.org/10.1016/j.engappai.2023.106957>

### **Outreach Efforts**

All experimental spray breakup data, including high-speed videos, processed velocity fields, and droplet size distribution measurements, will be made publicly accessible via [altjetfuels.illinois.edu](http://altjetfuels.illinois.edu).

### **Awards**

None.

### **Student Involvement**

This task has been primarily conducted by Casey O'Brien (PhD student).

### **Plans for Next Period**

The primary focus for the next period will be to complete the ROM of the multi-fuel spray data, which is the core of Task 2c. The DMD analysis, which is still in a preliminary stage (Figure 16), will be fully investigated. The objective is to move from initial findings of spatial coherence to a robust, predictive model that quantitatively links specific fuel properties (like viscosity) to the spatial growth rates of the dominant breakup instabilities.

Concurrently, the ignition analysis from Task 2b will be finalized. This involves correlating the flame kernel propagation dynamics (from broadband imaging, Figure 14) with the local, time-resolved droplet statistics (from X-ray PCI, Figure 13). This final step will provide a quantitative link between the evolving flame front and its direct impact on the local spray properties, completing the multi-modal ignition study.

### **References**

ASTM International. (2024). *ASTM D4054-24d: Standard Practice for Evaluation of New Aviation Turbine Fuels and Fuel Additives*. <https://doi.org/10.1520/D4054-24>

Leask, S., McDonnell, V., & Samuelsen, S. (2021). Modal extraction of spatiotemporal atomization data using a deep convolutional Koopman network. *Physics of Fluids*, 33. <https://doi.org/10.1063/5.0046177.80>

Jia, B., Xie, L., Deng, X., He, B., Yang, L., & Fu, Q. (2023). Experimental study on the oscillatory Kelvin-Helmholtz instability of a planar liquid sheet in the presence of axial oscillating gas flow. *Journal of Fluid Mechanics*, 959, A18.

<https://doi.org/10.1017/jfm.2023.19.81>

Kang, Z., Li, X., & Mao, X. (2018). Experimental investigation on the surface wave characteristics of conical liquid film. *Acta Astronautica*, 149, 15–24. <https://doi.org/10.1016/j.actaastro.2018.05.030>

Kasmaiee, S., Tadjfar, M., Kasmaiee, S., & Ahmadi, G. (2024). Linear stability analysis of surface waves of liquid jet injected in transverse gas flow with different angles. *Theoretical and Computational Fluid Dynamics*, 38, 107–38.

<https://doi.org/10.1007/s00162-024-00685-2.79>